

# A machine learning based approach for Groundwater mapping

Rashed Uz Zzaman<sup>1</sup>, Sara Nowreen<sup>1,\*</sup>, Irtesam Mahmud Khan<sup>2</sup>, Md. Rajibul Islam<sup>2</sup>, Nabil  
Ibtehaz<sup>2</sup>, M. Saifur Rahman<sup>2</sup>, Anwar Zahid<sup>3</sup>, Dilruba Farzana<sup>4</sup>, Afroza Sharmin<sup>5</sup>, M. Sohel  
Rahman<sup>2,\*</sup>

<sup>1</sup>*Institute of Water and Flood Management ,BUET, Bangladesh,*

<sup>2</sup>*Department of CSE, BUET, ECE Building, West Palashi, Dhaka-1205, Bangladesh,*

<sup>3</sup>*Bangladesh Water Development Board, Dhaka, Bangladesh*

<sup>4</sup>*Department of Public Health Engineering (DPHE), Dhaka, Bangladesh*

<sup>5</sup>*Bangladesh Agricultural Development Corporation, Dhaka, Bangladesh*

\*Corresponding Author:

Sara Nowreen & M. Sohel Rahman

BUET, Bangladesh

Email: [snowreen@iwfm.buet.ac.bd](mailto:snowreen@iwfm.buet.ac.bd); [sohel.kcl@gmail.com](mailto:sohel.kcl@gmail.com)

## Abstract

In Bangladesh, groundwater is considered to be the main source of both drinking water and irrigation. Suction lift pumps and force mode of operation are the predominant technologies for groundwater abstraction in Bangladesh. For a sustainable usage policy, it is thus important to identify which technology would be more appropriate in which area in Bangladesh. With that aim in mind, this paper proposes a methodology leveraging the power of machine learning (ML) that can potentially learn intricate relationships between the (annual maximum) groundwater level (GWL) and the relevant hydrogeological

24 factors (HGFs). A number of machine learning algorithms- both classification and regression models- have  
25 been trained. Our classification models are trained as a binary classifier to predict the abstraction technology  
26 of a particular point. Notably, our best classification model is based on the Random Forest algorithm, which  
27 has achieved an accuracy of 91% and an excellent value of 96% for the AuROC (Area Under Receiver  
28 Operating Characteristics Curve) indicating a strong discriminant capability thereof. We also identify  
29 (elevation derived from) Digital Elevation Model (DEM), Specific Yield and Lithology as the three most  
30 important HGFs for GWL in Bangladesh.

31 On the other hand, to predict the actual (annual maximum) groundwater level, we employ a two-stage  
32 approach, where we first employ the above-mentioned classification model to identify the suitable  
33 abstraction technology for the point of interest and subsequently predict the actual groundwater level using  
34 the appropriate Random Forest regressor and that too with reasonable accuracy (minimum absolute error is  
35 less than 1 for suction mode and less than 5 for the force mode). In the sequel, using our predictor models,  
36 we prepare groundwater (technology) maps for the whole Bangladesh.

37

38 **Keywords:** groundwater, hydrogeological factors, Machine learning, prediction, suction-mode pump,  
39 force-mode pump.

#### 40 **Article Highlights**

- 41 • A machine learning pipeline for predicting groundwater level (GWL) and abstraction  
42 technology is proposed.
- 43 • The relationship between the GWL and hydrogeological factors is learned by the proposed  
44 models.
- 45 • The most influential hydrogeological factors have been identified.
- 46 • Ground water (technology) maps for whole Bangladesh have been prepared.

47 **1. Introduction**

48 Groundwater, particularly at the shallow aquifers, is easily accessible, less vulnerable to pollution  
49 than surface water (Oke and Fourie 2017), and it is the most essential freshwater resource on the  
50 Earth. This underground resource is used mostly for domestic, agricultural, and industrial  
51 purposes. Almost 50% of megacities in the world and 80% of irrigation are reliant on groundwater  
52 (Bricker et al. 2017). The excessive use of groundwater is resulting in rapid depletion of  
53 groundwater level in the aquifer systems thereby creating a threat to the overall sustainability of  
54 worldwide water production (Dalin et al. 2018). As groundwater level is an initial indicator to  
55 estimate the groundwater quantity (i.e., the net annual recharge mostly for shallow aquifer which  
56 is estimated by water table fluctuation method), prediction of groundwater level may aid in the  
57 sustainable and effective management of groundwater resources (Hasda et al. 2020; Zhou et al.  
58 2017).

59 Currently, groundwater is the main source of both drinking water in irrigation in Bangladesh. In  
60 the early 1980s, groundwater-fed irrigation became widespread and number of shallow tube-wells  
61 (STW) (main source of groundwater supply) increased from 0.1 million to more than 1.5 million  
62 (Qureshi et al. 2014). During the past decades, Bangladeshi farmers gradually became more  
63 dependent on groundwater as most rivers and canals therein dried up during the dry season  
64 (December-May) (Harvey et al. 2006; Shahid 2008). Over-reliance on groundwater resulted in  
65 faster groundwater level depletion. Thus, various parts of Bangladesh face water stress,  
66 particularly, during the dry season. In this context, predicting groundwater abstraction technology  
67 as well as level could prove to be instrumental in sustainable groundwater management. With this  
68 brief backdrop, we propose a state-of-the-art machine learning based approach to predict  
69 groundwater abstraction technology and groundwater levels in Bangladesh.

70 There are a few studies in the literature that predict the groundwater level (GWL) principally using  
71 time series data and leveraging various soft computing techniques. For example, Husna et al.  
72 (2016) predicted the groundwater levels under different time intervals scenarios (i.e., one-week  
73 lead, five-week lead, ten-week lead, 15-week lead) using Artificial Neural Networks (ANN).  
74 Notably, their study was limited to Dawu Aquifer of Zibo in Eastern China. Very recently, Hasda  
75 et al. (2020) predicted the groundwater level in Bangladesh, albeit in a limited setting, focusing  
76 only on the Barind tract, situated in northwestern Bangladesh, covering only around 1942 km<sup>2</sup>  
77 area. In particular, Hasda et al. (2020) conducted a time series modeling employing a nonlinear  
78 autoregressive exogenous model (NARX) that was trained using the Bayesian Regularization (BR)  
79 algorithm. They used time series data containing weekly rainfall, temperature, humidity and  
80 evaporation during the period 1980–2017 to forecast GWL. Salem et al. (2018) conducted a study,  
81 again on a limited scale (i.e., only on a northwestern district of Bangladesh, namely, Rajshahi),  
82 where the goal was to analyze the effect of climate change on groundwater-dependent irrigation.  
83 As an intermediate output, Salem et al. (2020) predicted the GWL using a Support Vector Machine  
84 based model from the projected climactic variables. Salam et al. (2020) explored the relationship  
85 between groundwater level and El-Nino Southern Oscillation (ENSO) teleconnection indices  
86 during 1981–2017 in the northwestern region of Bangladesh covering 34600 km<sup>2</sup> area. As a sub-  
87 aim, they also predicted GWL changes from 2018 to 2025 leveraging ARIMA model. Another  
88 recent study by Hoque and Adhikary (2020) made an effort to predict GWL using the weekly GWL  
89 and rainfall data leveraging the power of ANN and autoregressive integrated moving average with  
90 exogenous variable (ARIMAX) time series models. However, their work is only limited to one of  
91 the western districts, namely, Kushtia.

92 While there are several studies attempting to predict GWL in Bangladesh (as discussed above),  
93 most of these studies leveraged historical time series data and or meteorological factors rather than  
94 investigating the relationship of GWL with factors influencing groundwater. The groundwater  
95 level is assumed to be intricately related to various hydrogeological factors (HGFs). For instance,  
96 influence of the thickness and permeability of the upper clay on GWL behavior has been discussed  
97 under National Water Management Plan (NWMP) study in Bangladesh (WARPO 2000). On the  
98 other hand, in Nowreen et al. (2021), various geospatial-based indicators like lineament density,  
99 drainage density, geomorphology, slope, lithology, soil, land use and land cover (LULC), and  
100 rainfall have been used to assess groundwater resources in the northwestern part of the country.  
101 Findings in recent study (Burgess et al. 2017) indicate the accuracy of the traditional borehole  
102 water level measurement as a means to monitor groundwater storage and recharge on the largest  
103 fluvio-deltaic aquifer system including the Bengal Delta. However, the intricate relationship  
104 between and among these hydrogeological factors and the actual groundwater level has not been  
105 hitherto investigated, particularly in the context of predicting GWL. This research gap, particularly  
106 in the context of Bangladesh is addressed in this work. Also, most of previous works are limited  
107 to a particular area of Bangladesh whereas we here present a country-wide study. Thus, our  
108 objective revolves around developing yet another machine learning based model to predict the  
109 groundwater level, albeit through taking a detour from the already published works that have  
110 mostly focused on time series data and meteorological factors for such predictions and focusing  
111 on different hydrogeological factors (i.e., slope, elevation, drainage density, lithology, specific  
112 yield etc.) as influential factors for groundwater. This paper makes the following key contributions:

- 113 1. We propose a methodology and develop a model leveraging the power of machine learning  
114 (ML) techniques to learn the intricate relationships between the GWL and different  
115 hydrogeological factors (HGFs).
- 116 2. We further identify the most influential factors among the 14 HGFs considered in this  
117 study. Our research reveals that (elevation derived from) Digital Elevation Model, specific  
118 yield and lithology are the three most important HGFs influencing groundwater in  
119 Bangladesh. To the best of our knowledge, this is the first study to identify such important  
120 pieces of knowledge thereby extending the knowledgebase of understanding groundwater  
121 recharge in Bangladesh.
- 122 3. In Bangladesh, two predominant pumping modes/technologies (popularly referred to as  
123 groundwater technology), namely, Suction (S) and Force (F) are used for groundwater  
124 abstraction. We use our developed ML based (classification) models (using the most  
125 influential HGFs) to identify which pumping modes/technology would be appropriate in  
126 which area of Bangladesh with promising accuracy.
- 127 4. We further develop regression models, again based on the most influential HGFs, to predict  
128 the actual values for the GWL through a two-step pipeline for better accuracy.
- 129 5. Finally, we produce the groundwater (technology) map (i.e., a map identifying the  
130 appropriate abstraction technology) for the whole Bangladesh. In particular, we prepare a  
131 2×2km resolution map for Bangladesh where each grid point is identified using our ML  
132 based model as either S (i.e., appropriate for suction mode of operation) or F (i.e.,  
133 appropriate for force mode of operation). We also prepare a map at the same resolution  
134 where the predicted GWL values have been plotted. To the best of our knowledge, this is

135 the first attempt to prepare a country-wide groundwater technology map as well as GWL  
136 map at such a high resolution.

## 137 **2. Methods**

138 Our methodology evolves around trying to capture this intricate relationship between and among  
139 the HGFs and GWL through the power of machine learning. Our goal is to be able to infer for any  
140 point, which technology (suction vs. force) would be appropriate. Informatively, suction mode  
141 abstraction works when the vertical distance between the centrifugal pump and pumped water level  
142 depth is within 7.5 meters; on the other hand, when the pumped water level depth is more than 7.5  
143 meters, we need to apply force mode abstraction. Now, our main idea is as follows. Assume that  
144 we have the GWL data labelled as either S (i.e., suction) or F (i.e., force) and HGFs data for a  
145 number of points (referred to as representative points hence forth). We can then train a machine  
146 learning model as a binary classifier (S vs. F) using the data of these representative points where  
147 the HGFs are treated as features.

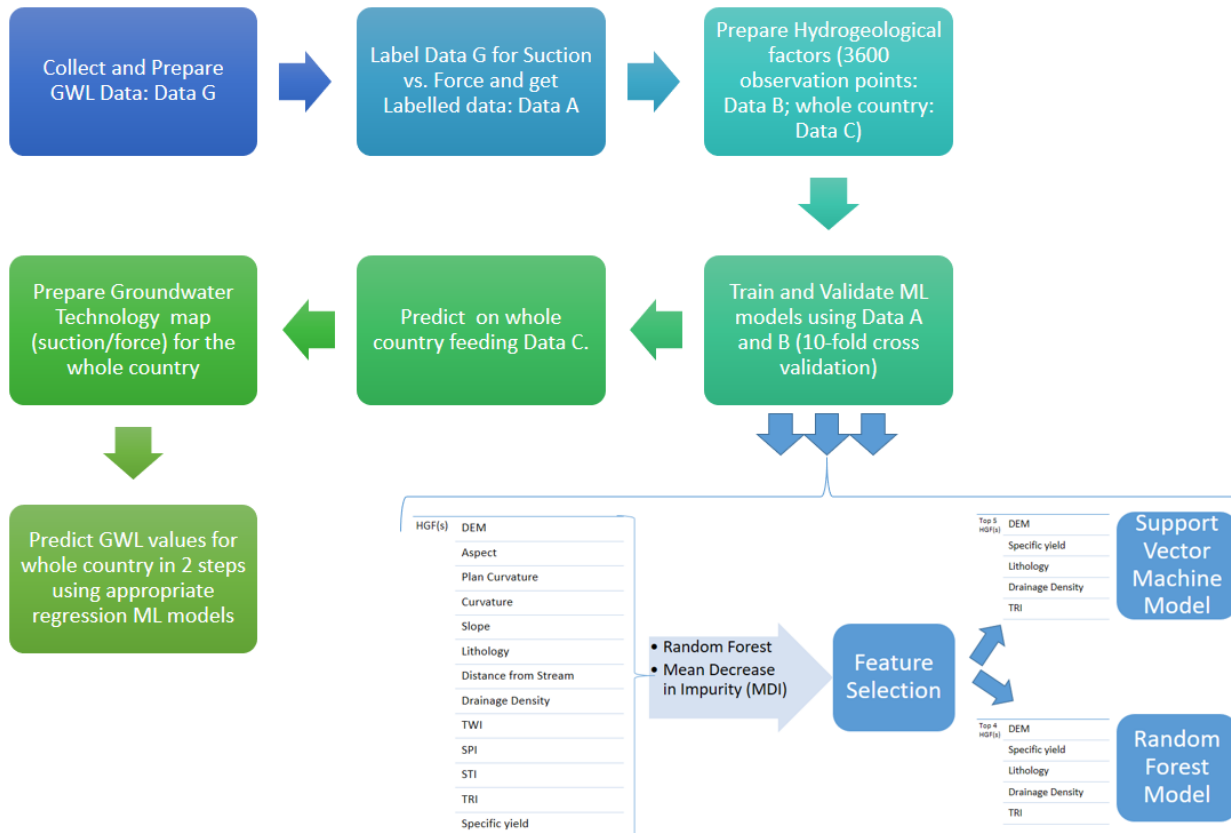


Figure 1: Overall methodology and the machine learning pipeline.

148

149 If there are enough and diversified representative points, we can hope that the model will  
 150 generalize and successfully learn the intricate relationship we want it to learn. Note that, here first  
 151 we work on a binary classification problem, where the goal is to infer one of the two classes: S or  
 152 F. Subsequently, we develop regression models to handle a more difficult problem of inferring the  
 153 actual ground water levels. To this end, for better accuracy, we employ a two-stage pipeline as  
 154 follows. We train two regression models, tailored to do well in areas labelled as S and F  
 155 respectively. When the models are ready, we first use our (binary) classification model to predict  
 156 the point of interest as either S or F. Based on the prediction, we then employ the appropriate  
 157 regression model to predict the groundwater level. Figure 1 shows the overall research workflow.



## 158 *2.1 Study Area and Datasets*

159 The study area of this research is whole Bangladesh and the target is shallow aquifers most of  
160 which are unconfined with Holocene deposits with only a few part thereof (~18%) exhibiting semi  
161 confined nature for its Pre-Holocene condition (see Figure 2). Thus the principal focus of this study  
162 is shallow (unconfined) aquifers where net impact of groundwater stress (either due to less  
163 recharge or more discharge) is identifiable by groundwater position (or declination). Lower  
164 aquifers are typically located within 10-60 m depth (Ravenscroft et al., 2005) and replenished  
165 annually, except in the capital, Dhaka where a significant cone of depression is observed with  
166 water table depths of 15 m to 35 m. Outside of Dhaka, seasonal fluctuations are typically up to 8  
167 meters but spatially vary depending on local hydrogeology and groundwater withdrawal  
168 (Shamsudduha et al. 2009).

169 Nationally ~1,400,000 and ~38,000 suction mode and force mode based pumps, respectively  
170 withdraw groundwater through irrigation abstraction wells (BADC, 2019). But, suction mode  
171 pumps fail when maximum GWL depletes more than 7.5 meters (i.e., the vertical distance between  
172 the centrifugal pump and the pump valve is more than 7.5 meters) . That is why the latest available  
173 observation points on annual maximum groundwater level is used to facilitate government  
174 organizations to prepare policy trajectories for upcoming years. With this in mind, we consider  
175 annual maximum groundwater level (GWL) values that occur in April in this study.

176 Quality assured monitoring observation points of annual maximum groundwater level (GWL) for  
177 the year 2018 have been screened from the data collected from different sources, namely,  
178 Bangladesh Water Development Board (BWDB) (726 out of 1124 monitoring boreholes),  
179 Bangladesh Agriculture Development Corporation (BADC) (2435 out 3164 observation wells) and  
180 Department of Public Health and Engineering (DPHE) (414 out of 4831 observation wells) and

181 Barind Multipurpose Development Authority (BMDA) (25 out of 25 monitoring boreholes). Based  
 182 on the GWL values, each of these 3600 points has been labelled as either S (i.e., appropriate for  
 183 suction mode abstraction) or F (i.e., appropriate for force mode abstraction).

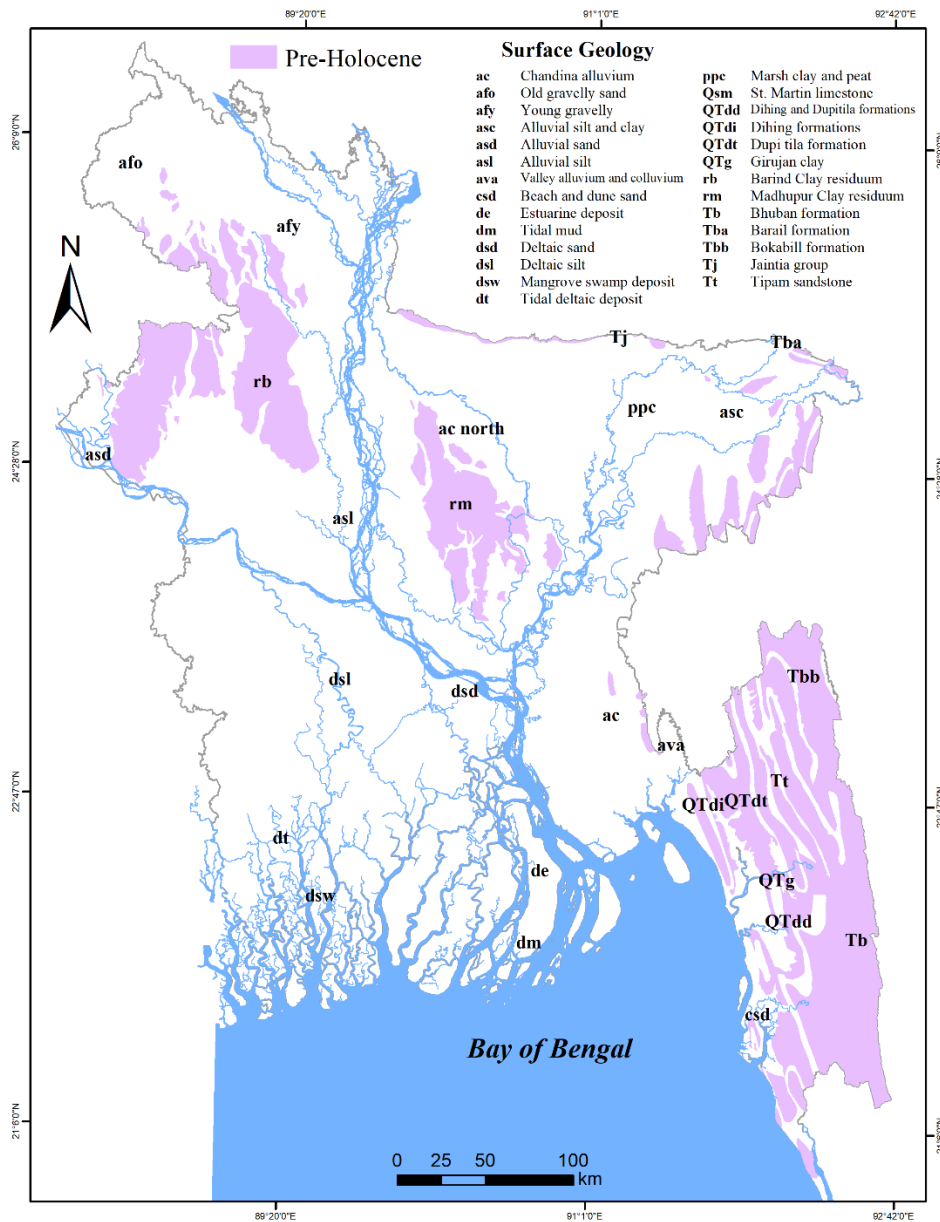


Figure 2: Surface Geology of Bangladesh

184

185

186 **2.2 Preparation of hydrogeological factors**

187 Through detailed literature study, a total of fourteen hydrogeological factors-HGFs, namely,  
188 Digital Elevation Model (DEM), Curvature, Plan Curvature, Aspect, Slope, Distance from Stream,  
189 Lithology, Drainage Density, Stream Power Index (SPI), Sediment Transport Index (STI), Terrain  
190 Roughness Index (TRI), Topographic Wetness Index (TWI) and Specific yield (Sy) have been  
191 identified that are believed to have intricate relationship with the groundwater level. Specific yield  
192 data was collected from BWDB and an interpolated surface was generated using the interpolation  
193 technique. Then we proceed as follows.

194 Freely available lithology map was collected from United State Geological Survey (USGS) (Alam  
195 et al. 1990) and subsequently, geo referencing of this map was done in ArcGIS environment. The  
196 geo referenced lithology map was digitized to create polygon shapefiles and finally, polygon  
197 shapefiles were converted into the raster format in 30m resolution. Digital elevation model (DEM),  
198 of 30m resolution, was collected from USGS website (“Earth Resources Observation and Science  
199 (EROS) Center” 2021). Notably, elevation has indirect impacts on the groundwater level, as higher  
200 elevations have higher slope in our study area which falls into the Hindu Kush Himalayan Region  
201 and decreases the infiltration rate (Althuwaynee et al. 2014). Aspect is related to the exposure to  
202 sunlight (Lee et al. 2001) and hence has impact over evaporation. Elevation and aspect maps were  
203 generated form DEM data using ArcGIS. Slope significantly influences water infiltration and  
204 surface runoff (Sarkar et al. 2001). Therefore, we generated the slope map using Equation 1  
205 (below) (Machiwal et al. 2011) in ArcGIS.

206 
$$Slope = 100 \times \frac{\sqrt{AX^2 + BY^2}}{Pixel\ Size\ (DEM)} \dots\dots\dots (1)$$

207 Here, AX (BY) = filtered DEM with x-gradient (y-gradient) filter.

208 Curvature represents the topography and morphology of the earth surface. It is composed of three  
 209 aspects, namely, plan, profile and total. Now, the profile and plan curvature mainly impact  
 210 acceleration and deceleration of flow on the ground surface (Al-Abadi et al. 2016). The plan,  
 211 profile, and total curvature maps of were generated in ArcGIS using Equation 2.

212 
$$K = \left| \frac{dT}{ds} \right| \dots\dots\dots (2)$$

213 Here,  $T$  is a unit of tangent vector,  $ds$  is a differential of the curves length and  $|\bullet|$  denotes the  
 214 magnitude of the vector.

215 To generate the drainage density and distance from stream maps, initially the drainage network of  
 216 was extracted from DEM (30m resolution) by using ArcGIS. The derived drainage network is  
 217 subsequently used to calculate the drainage density ( $dd$ ) (Razandi et al. 2015) and distance for  
 218 stream ( $d_{ij}$ ) using Equations 3 and 4, respectively.

219 
$$dd = \frac{\sum_{i=1}^n D_i}{A} \dots\dots\dots (3)$$

220 Here,  $dd$  is the drainage density ( $km/km^2$ ),  $D_i$  is the total length of streams and  $A$  is the grid area  
 221 ( $km^2$ ).

222 
$$d_{ij} = \sqrt{\sum_{k=1}^n (X_{ik} - Y_{jk})^2} \dots\dots\dots (4)$$

223 Here,  $d_{ij}$  represents the distance from stream for  $i, j$  locations and  $k$  means features.

224 SPI estimates the degree of slope erosion owing to flowing water at a specific location of the basin  
 225 area. STI measures the sediment transport capacity of overland flow using slope steepness and

226 slope length (Wischmeier and Smith 1978). Following (Sameen et al. 2019), SPI and STI factors  
 227 were computed using Equations 5 & 6, respectively.

228  $SPI = A_s \times \tan \beta$  ..... (5)

229  $STI = \left(\frac{A_s}{22.13}\right)^{0.6} \times \left(\frac{\sin \beta}{0.0896}\right)^{1.3}$  ..... (6)

230 Here,  $A_s$  is the specific catchment area per unit contour length ( $m^2/m$ ) and  $\beta$  is slope angle (in  
 231 degrees).

232 Other influencing factors, namely, TRI and TWI were calculated using Equations 7 & 8,  
 233 respectively (Sameen et al. 2019).

234  $TRI = \sqrt{max^2 - min^2}$  ..... (7)

235  $TWI = \ln\left(\frac{A_s}{\beta}\right)$  ..... (8)

236 Here,  $A_s$  and  $\beta$  are same as in Equation 6, and  $max$  and  $min$  are the highest and lowest cell values  
 237 in the DEM.

238 **2.3 Groundwater abstraction classification using Machine Learning Models**

239 We propose a machine learning (ML) model to classify a point/area (based on the GWL) as  
 240 characterized by either suction-lift (S) of force-lift (F) abstraction. We have considered the 14  
 241 HGFs for this purpose. Figure 1 briefly presents an overview of our machine learning pipeline,  
 242 which will be further explained in the next subsections.

243

### 244 *2.3.1 Selection of Features*

245 It is important to choose features that have strong discriminatory capabilities with respect to  
246 classification task at hand as this may have profound effects on the performance thereof. Mostly  
247 two types of approaches for feature selection are found in the literature, namely, the filtering and  
248 wrapper approach; here we use the former, where a machine learning algorithm (independent of  
249 the choice of the actual learning algorithm to do the classification task) is leveraged for feature  
250 selection purposes. To this end, we have used the random forest (RF) classifier algorithm for  
251 ranking the features. RF algorithm, developed by Breiman (2001), is a nonparametric learning  
252 algorithm that generates many classification trees by bootstrap samples thereby attempting to  
253 improve the prediction performance. We have used Mean Decrease in Impurity (MDI) as the  
254 ranking criterion. MDI refers to the mean total decrease (considering all trees) in node impurities  
255 from splitting on the variable. The node impurity is measured by a statistical measure of  
256 distribution, namely, Gini index. Higher value of MDI indicates a better feature.

257 Once all the features are ranked, we try to find the best subset of features for our classification task  
258 at hand. We proceed iteratively as follows. We take the most important feature and train (through  
259 cross validation) and evaluate our models. Then we extend our feature set by including the second  
260 most important feature and so on. For each feature set we have trained our model with several  
261 classifiers such as Random Forest, Support Vector Machine (SVM) etc.. Based on different  
262 evaluation metrics discussed later on this section, we have found the best subset of features.  
263 Notably, we have also used R package ‘leaps’ (Lumley and Lumley 2013) for finding the best  
264 subset of features. However, ranking with random forest seems to have served our purpose better.

### 265 **2.3.2 Training the Classification Model**

266 We have trained our model with different classifiers and have applied  $K$ -fold cross validation,  
267 where the training dataset is first partitioned into  $K$  equal-sized subsets in order to subsequently  
268 train the model with  $K-1$  subsets and test it with the remaining subset, repeating this train-test  
269 procedure  $K$  times ensuring that the model is tested against each subset exactly once. In the  
270 literature, the popular choice for  $K$  is 10 which we follow here(Kohavi 1995).

271 Class imbalance can turn out to be a crucial issue in the context of Machine Learning which is also  
272 present in our case as 2413 points are labelled as S (suction-lift) and 1187 points as F (force-lift).  
273 Such imbalance in the training data may create a bias in favour of the majority class (i.e., S points).  
274 So, in addition to experimenting with the original (imbalanced) instances, we also conducted  
275 experiments after applying a popular sampling scheme, called SMOTE (Synthetic Minority Over-  
276 sampling Technique) (Chawla et al. 2002) on the training dataset thereby oversampling the  
277 minority class. However, the results did not change much suggesting that adequate minority class  
278 instances were available in the dataset.

### 279 **2.4 Groundwater level prediction using Regression Models**

280 Following the classification task through the machine learning pipeline presented in the above  
281 section, a regression task is also performed to predict the actual value of GWL. Here the goal is to  
282 train a machine learning (regression) model using the HGFs as features that can predict the actual  
283 ground water level given the HGFs of the respective area/point. For better performance, two  
284 separate regression models (i.e., S-Model and F-Model) are trained based on the two abstraction  
285 classes (i.e., S and F). So, the goal is to utilize the regression model in a two-step setting: first the  
286 classification model is used to classify (using our classification model) whether the area/point

287 under consideration is characterized by suction or force mode abstraction and subsequently  
288 leverage the appropriate regression model (i.e., S-Model or F-Model) to predict the GWL value.

289 The regression pipeline also uses the feature selection step. In particular, our regression models  
290 are trained based on the top ranked four features as found through our feature ranking exercise for  
291 the classification task. Informatively, any categorical variable is converted to one-hot-encoded  
292 vectors following standard procedure. Furthermore, the feature vectors are mean normalized, i.e.,  
293 normalized to have zero mean with unit variance.

294 A number of regressor models (Freedman 2005), namely,  $K$ -Nearest Neighbor (KNN) regressor,  
295 Random Forest regressor, Support Vector Regressor (SVR), Adaboost regressor, Neural Network  
296 regressor, etc. have been experimented with. We also have performed an ensemble of the models  
297 by taking their prediction and fitting a linear regressor with elastic net regularization (Zou and  
298 Hastie 2005). Finally, based on the Minimum Absolute Error (MAE) performance measure as well  
299 as qualitative inspection of the produced groundwater map, the Random Forest regressor is chosen  
300 as the main regressor model. As has been mentioned above, two separate models, namely, S-Model  
301 and F-Model, have been trained- one considering the points labelled as S (i.e., having Suction-lift  
302 abstraction characteristic) and the other with the points labelled as F (i.e., having Force-lift  
303 abstraction characteristic). This makes sense as there are significant characteristic differences  
304 between the two sets of points (which was also reflected from significantly worse performance  
305 when training was done as a single model considering all points together). The models have been  
306 trained following a  $K$ -fold ( $K = 10$ ) cross validation scheme. The number of estimators for the  
307 Random Forest regressor have been set (through a grid search) to 70 and 100 for the S-Model and  
308 F-Model respectively.



## 309 **2.5 Evaluation Metrics**

310 To evaluate the performance of the classification models, we have used well-established and  
311 popular performance metrics from the literature (Altman and Bland 1994; Powers 2020), namely,  
312 accuracy, sensitivity, specificity, F1 score, Precision and Matthew's correlation coefficient (MCC).  
313 These performance metrics are calculated using the following equations:

$$314 \quad Accuracy (Acc) = \frac{TP + TN}{P + N}$$

$$315 \quad Sensitivity (Sn) = \frac{TP}{TP + FN}$$

$$316 \quad Specificity (Sp) = \frac{TN}{FP + TN}$$

$$317 \quad Precision = \frac{TP}{TP + FP}$$

$$318 \quad Recall = \frac{TP}{TP + FN}$$

$$319 \quad MCC = \frac{TP * TN - FP * FN}{\sqrt{(TP + FN)(TP + FP)(TN + FP)(TN + FN)}}$$

$$320 \quad F1 = \frac{2 * Precision * Recall}{Precision + Recall}$$

321 Here,  $P$ ,  $N$ ,  $TP$ ,  $TN$ ,  $FP$ ,  $FN$  respectively denote the number of positives, negatives, true positives,  
322 true negatives, false positives and false negatives.

323 We have also analyzed the ROC-Curve, i.e., the area under receiver operating characteristic curve  
324 (ROC-Curve) (Fawcett 2006) and the PR-Curve, i.e., area under precision-recall curve (Davis and  
325 Goadrich 2006). These two measures in combination can accurately reflect the performance of a

326 predictor particularly in the context of imbalance in the dataset. To get the ROC-Curve, we need  
327 to plot, at various threshold settings, the true positive rate (TPR), i.e., Sensitivity against the false  
328 positive rate (FPR), i.e.,  $(1 - \text{Specificity})$ . A ROC-Curve closer to the upper-left corner indicates  
329 better performance (Fawcett 2006) and gives a higher (desirable) value for auROC, i.e., the area  
330 under the ROC-Curve. To draw the PR-curve we plot, at various threshold settings, the precision  
331 against the recall. A PR-curve closer to the upper-right corner indicates better performance of the  
332 predictor (Davis and Goadrich 2006) and gives a higher (desirable) value for the auPR, i.e., the  
333 area under PR-Curve.

334 For the regression task, we have used Mean Absolute Error (MAE) as the main performance metric  
335 along with the standard deviations. MAE measures the errors between paired observations that  
336 express the same phenomenon and is calculated using the following equation:

$$337 \quad MAE = \frac{\sum_{i=1}^n |y_i - x_i|}{n} = \frac{\sum_{i=1}^n |e_i|}{n}$$

338 In other words, MAE is the mean of the absolute errors,  $|e_i| = |y_i - x_i|$ , where  $|y_i|$  and  $|x_i|$  refer  
339 to the prediction and the true value, respectively.

### 340 **3. Results**

#### 341 ***3.1 Groundwater abstraction technology classification***

342 Among all the classifiers we have implemented, the best performers turned out to be RF and SVM.  
343 We conducted 10-fold cross validation for both of them. The decision threshold was assumed to  
344 be 0.5. Table 1 reports the results.

345

346

347

Table 1: Classification performance (on different metrics) of the best models

Classifier	# Features	auROC	auPR	Accuracy	Specificity	Sensitivity	F1 Score	MCC	Precision
Random Forest	4	0.96	0.91	0.91	0.94	0.85	0.86	0.80	0.88
SVM	5	0.90	0.78	0.83	0.92	0.63	0.70	0.59	0.79

348

349 For Random Forest and SVM, best number of features are 4 and 5 respectively. Random Forest  
 350 performs a bit better than SVM. Another important observation is that Random Forest provides a  
 351 more balanced result as compared to SVM.

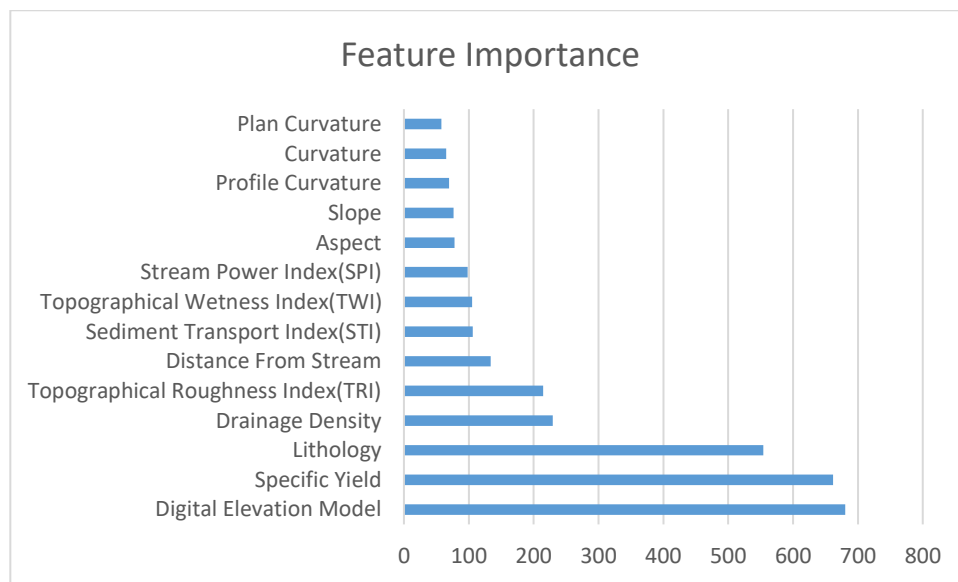


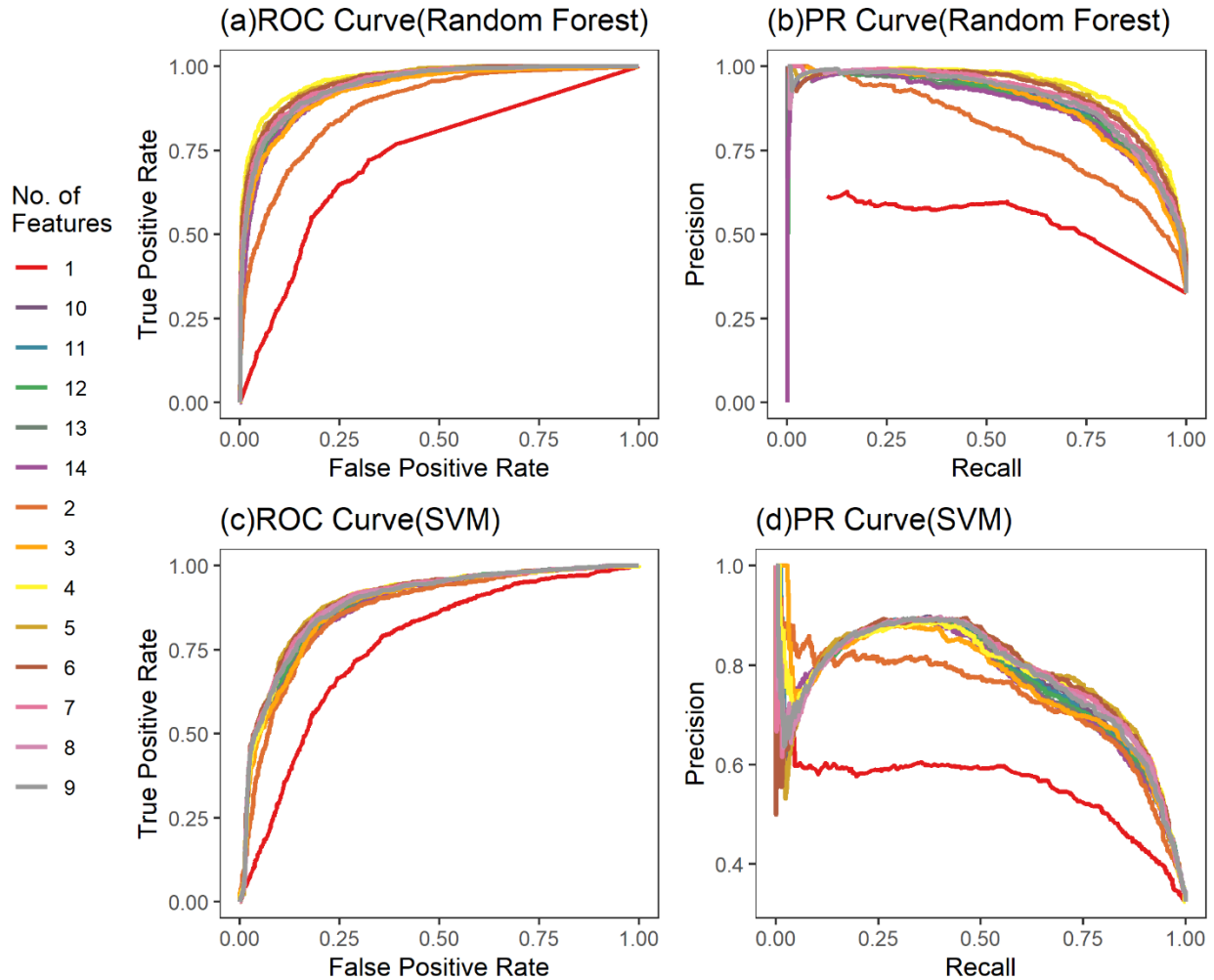
Figure 3: Feature (HGFs) Importance Based on MDI

352

### 3.2 Feature Importance

353 Considering the classification task, we ranked all the features based on Mean Decrease Impurity  
 354 (MDI) of Random Forest algorithm (Figure 3). We can see that, Digital Elevation Model (DEM)  
 355 is the most important feature for classification. It is particularly true as elevation affects only  
 356 renewable (i.e., net annual) recharge part of shallow aquifers of the study under investigation.  
 357 Also, DEM is closely followed by the Specific Yield (Sy) and Lithology. We further observe that

358 the last few features (e.g., different curvatures) do not have much of an impact on the classification  
 359 task. Mostly, the top four-five features are sufficient to predict the target.



360

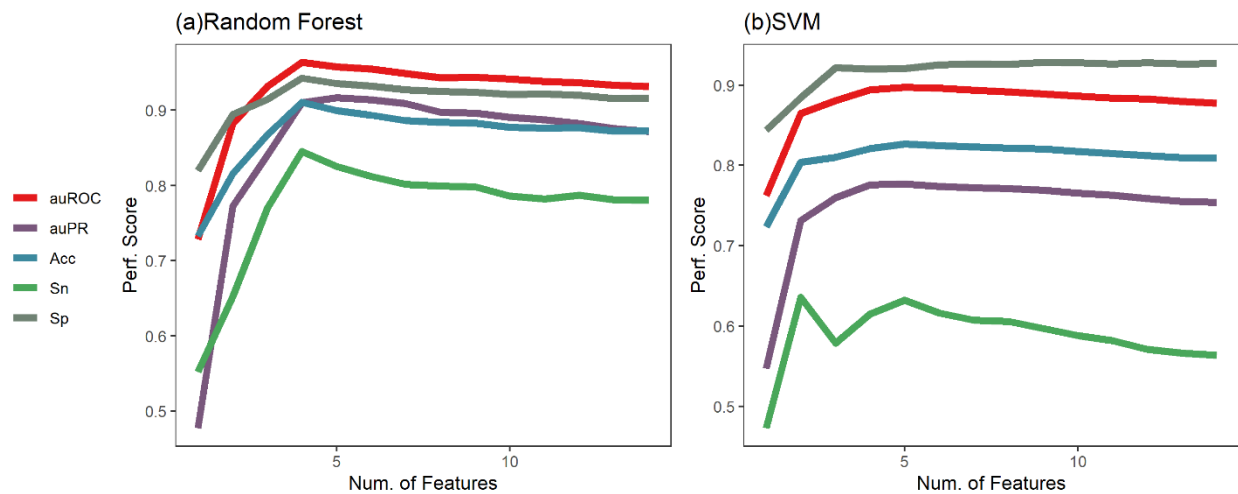
361 Figure 4: ROC-Curves and PR-Curves for Random Forest and SVM classifiers considering  
 362 incremental subset of features based on feature ranking. (a) ROC-Curves for Random Forest (b)  
 363 PR-Curves for Random Forest (c) ROC-Curves for SVM (d) PR-Curves for SVM.

364

### 365 *3.3 Impact of Number of Features*

366 To assess the impact of the number of features on the classifier performance, in Figure 4, we plot  
 367 the ROC-Curves and PR-Curves for both RF and SVM. In each case, 14 different curves are  
 368 generated as follows: we started with only the most important feature (c.f. Figure 3) and augmented

369 the feature set incrementally by adding the next ranked features one by one. Evidently (c.f. ROC-  
 370 Curves of Figure 4 (a) and (c)), if we increase the number of features, we notice significant  
 371 performance improvement at a good rate initially (particularly up to 4 features). Subsequently  
 372 however, the improvement is not that noticeable i.e., the curves for 4 to 14 features are almost  
 373 similar. We also analyze the PR-Curve as for imbalanced datasets, ROC-Curve alone is not  
 374 adequate to assess the impact of selected features; rather PR curve is more relevant in this context  
 375 (Davis and Goadrich 2006). From the PR-Curves as well (Figure 4 (b) and (d)), we reach the same  
 376 conclusion.



377  
 378 Figure 5. Classifier Performance against different number of features. Performance metrics include  
 379 area under ROC and PR curves (auROC and auPR), accuracy (Acc), Sensitivity (Sn), Specificity  
 380 (Sp) and F1 Score (F1). Perf. Score indicates the metric value for a particular performance metrics.  
 381 (a) Random Forest Classifier performance (b) SVM Classifier performance.

382  
 383 We also have plotted the auROC, auPR, accuracy, sensitivity and specificity values for both  
 384 Random Forest and SVM models that use varying number of top-ranked features (Figure 5). Like  
 385 the ROC-Curves and PR-curves, increasing number of features seems to improve all the  
 386 performance measures albeit up to a certain point, after which, that performance either decreases  
 387 or gets saturated. Evidently, the best results are achieved using the top 4-5 features.

388 **3.4 Regression results for GWL values**

389 Our Random Forest regressor models, namely, S-Model and F-Model, are trained based on the top  
390 ranked four features as found through our feature ranking exercise for the classification task  
391 (Figure 3). These features are: digital elevation model (DEM), specific yield (Sy), lithology and  
392 drainage density. Lithology, being a categorical variable is converted to one-hot-encoded vectors  
393 following standard procedure. The model performances are presented in Table 2.

394 Table 2: Regression Performance in MAE of our Random Forest regressor models.  $x \pm y$  means  
395 MAE is x with standard deviation y.

Model	Performance	Comment
S-Model	$0.949 \pm 0.05$	Applicable for Suction-Lift abstraction points
F-Model	$4.296 \pm 0.707$	Applicable for Force-Lift abstraction points

396

397 **3.5 Groundwater (technology) maps for Bangladesh**

398 With the groundwater abstraction (suction-lift vs. force-lift) classification model at hand, we now  
399 produce the Ground Water Technology map for whole Bangladesh, which each point/area of the  
400 country is identified as having either suction-lift or force-lift abstraction characteristics. To this  
401 end, we divided Bangladesh into 2×2km resolution grid as Brammer (2012) reports that, in  
402 Bangladesh, there is minimal hydrogeological variation within such a grid. Here, the center point  
403 of each grid was used to extract the HGFs values. The extracted HGFs values are particularly  
404 chosen from the majority categorical classification of every 2x2km grid using the majority  
405 statistical technique known as zonal statistics tool in ArcGIS platform. In fact, we do not need all  
406 the HGFs values, we only use the top ranked 4 features (c.f. Figure 3), namely, digital elevation

407 model (DEM), specific yield (Sy), lithology and drainage density (notably, if we decide to run the  
408 SVM model we would also need TRI). Subsequently, we have run our Random Forest  
409 classification model to produce the Groundwater Technology map for Bangladesh (Figure 6). We  
410 have also produced a map where the groundwater level values are presented. To this end, we have  
411 used our Random Forest Regressor models (i.e., S-Model and F-Model) in combination with our  
412 Random Forest Classification model as follows. As has been presented in Figure 6, our Random  
413 Forest Classification model has predicted each 2×2km resolution point as either S (Suction-mode)  
414 or F (Force-mode). If a 2×2km resolution point is labelled as S, we predict the value of GWL using  
415 the S-Model and otherwise (i.e., if it is labelled as F) we use the F-Model. Figure 7 presents the  
416 resulting map (GW-Map).

#### 417 **4. Discussions**

418 High resolution quality data is a prerequisite for proper planning and designing in any sector. To  
419 this end, hydrological data collected by BWDB is definitely useful for sustainable water  
420 management in Bangladesh. However, the pertinent question in this regard is whether the  
421 hydrological data collection network density for the area under consideration satisfies the standard  
422 resolution. For Bangladesh, this is certainly lacking: resolution of the groundwater observation  
423 well network in the country is about 77km<sup>2</sup> against the standard resolution of 5-20/km<sup>2</sup> (Hossain,  
424 M and Zahid 2014). This is inadequate for sustainable groundwater planning and management at  
425 the village, or even union (lowest administrative unit) level. High resolution data prediction using  
426 machine learning based approaches can fill this gap in this regard.

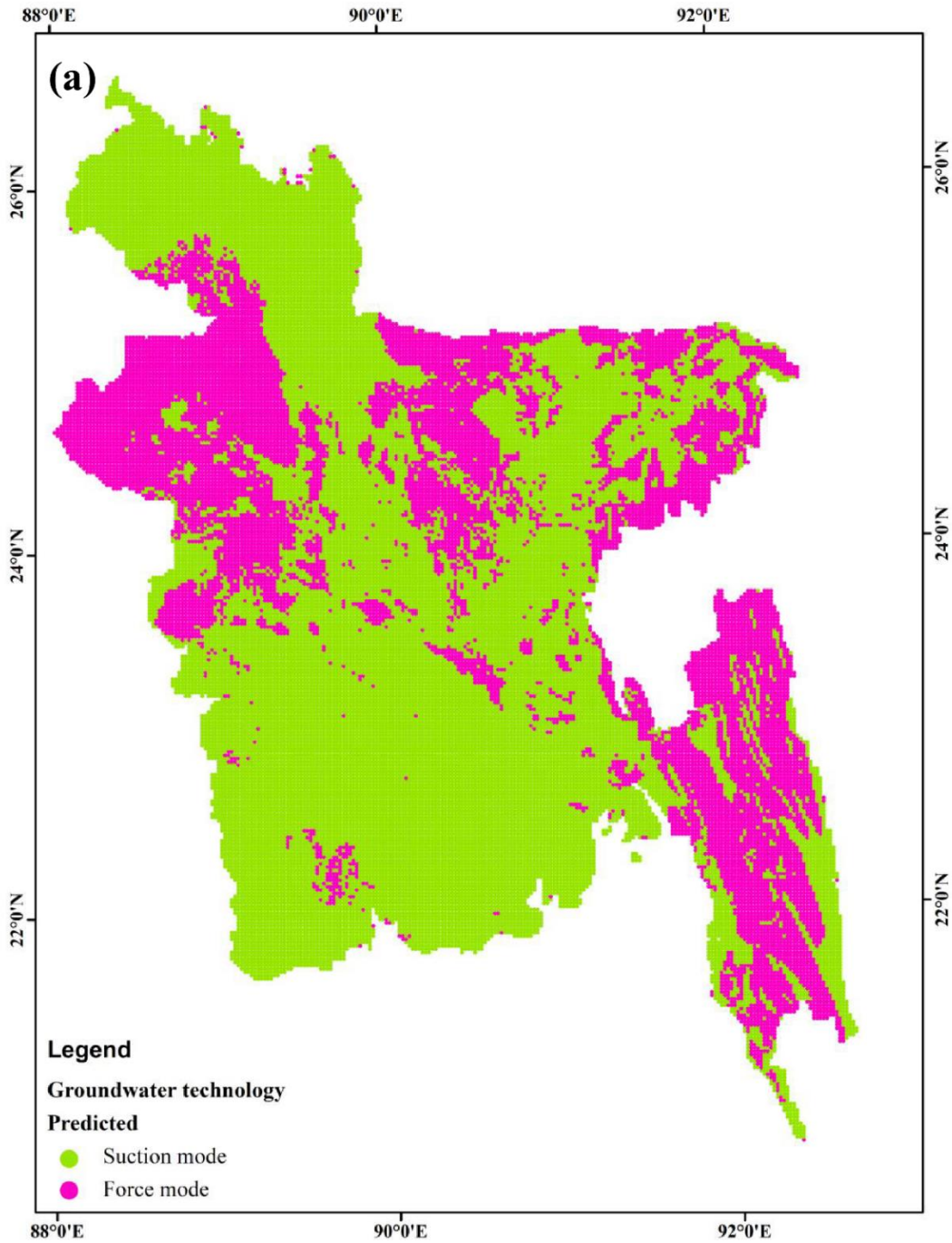


Figure 6: Groundwater (technology) map for Bangladesh. Here suction-mode and force-mode abstraction characteristics have been predicted using our Random Forest classification model in 2×2km resolution grid.



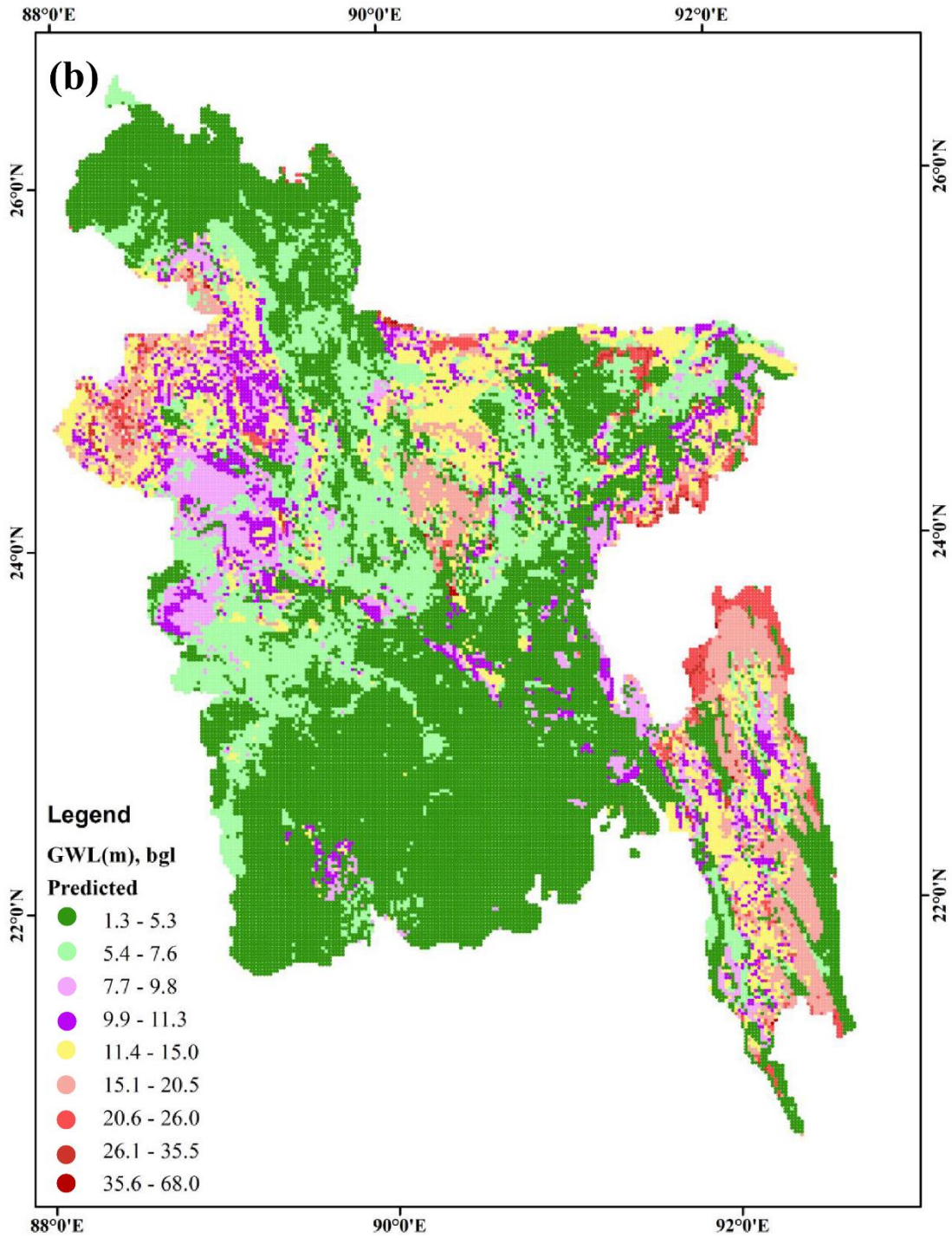


Figure 7: Groundwater map (GW-Map) for Bangladesh. Here annual maximum GWL values that occur in April have been predicted using our Random Forest classification and regressor models in 2×2km resolution grid.

428

429

430 We have leveraged the power of machine learning (ML) models that can potentially learn the  
431 intricate relationship between the ground water level (GWL) and the relevant hydrogeological  
432 factors (HGFs). A number of studies in the literature have investigated (using different  
433 methodologies and approaches) and identified important influencing factors for groundwater. In  
434 our research, elevation (DEM) and specific yield (Sy) have been found to be the most influential  
435 factors, which are closely followed by lithology. Our findings are in line with that of Arabameri et  
436 al. (Arabameri et al. 2020) as they also found lithology and elevation as highly influential. Also, it  
437 is well-perceived that in the flood plain, the lithological formation has a big impact rather than  
438 other indicators. On the other hand, hilly area indicators are mostly influenced by elevation and  
439 slope. Notably, various studies (e.g., Abdollahi et al. 2019; Miraki et al. 2019; Nguyen et al. 2020))  
440 found groundwater aquifer, land use, and TWI as influential factors. Also, LULC, lithology, and  
441 elevation were found to be more influential Arabameri et al. (Arabameri et al. 2020). Since 80%  
442 of Bangladesh (i.e., our study area) constitute flat area, slope and slope related factors (i.e, TWI,  
443 TRI, SPI, and STI) have been found to be less influential. Notably, our selected HGFs already  
444 represent the main parts of LULC and hence it is not considered separately in our study.

445 Using our classification model, we have produced a groundwater technology map for Bangladesh  
446 where, in 2×2km resolution, we have predicted each point as having either suction-mode of force-  
447 mode abstraction characteristic. Deeper groundwater levels are found to be significantly  
448 influenced by impermeable lithology characters, i.e., Barind Clay residuum, Madhupur Tract and  
449 hard/rocky layers of the hilly eastern region. In fact, these are the locations where suction mode  
450 pumping is usually failing during the dry months (March-April). So extra precaution is always  
451 needed before allowing further irrigation expansion with force modes in such areas. From  
452 hydrogeological point of view, these sites demand some counteractive actions to prevent recharge

453 loss and avoid groundwater overexploitation (Nowreen et al. 2021). Our produced map therefore  
454 could be instrumental in forming and enforcing a sustainable policy in this regard.

455 Additionally, we have used regression models to predict groundwater levels for Bangladesh. In  
456 Figure 7, we present the GWL spatial distribution map of Bangladesh. Because of the lack of  
457 infiltration of rainwater, the groundwater level is deeper in a few specific regions (e.g., Barind and  
458 Dupi Tial formation) in Bangladesh. This can be attributed to the low transmissivity (in the range  
459 of 500–2,000 m<sup>2</sup>/day) at the Dupi Tila aquifer system (EPC/MMP 1991) as opposed to the much  
460 higher transmissivity (in the range of 3,000– 5,000 m<sup>2</sup>/day) at similar depths in the flood-plain  
461 Holocene aquifer. GWL is more than 60m BGL (below ground level) in Barind and Dupi Tila  
462 formation, which has been captured by our regression model as is evident from some red dots in  
463 and around that region. On the other hand, the coastal areas are formed by the recent deltaic  
464 formation and groundwater levels in these areas are found to be near from the surface between 0  
465 to 4m. This has also been captured well in our model (Figure 7).

466 In general, hydrologists commonly predict GWL in unsampled sites by interpolation methods  
467 available in the GIS platform, most widely the Ordinary Kriging (OK) method. Now, prediction  
468 error variance for the OK method becomes larger where local variability is greatly varied with  
469 space, in particular in complex hydrogeological environment (Yamamoto 2000). Figure 8 presents  
470 a map (OK-GW-Map) illustrating the spatial distribution of groundwater level all over the country  
471 employing Ordinary Kriging using the same training samples used in our ML based approach.  
472 Evidently, the OK-GW-Map failed to capture such complex phenomenon in areas like Dhaka  
473 (Dupi Tila formation), Barind and Chittagong Hill Tracts (CHT) of Bangladesh which is well-  
474 captured in the GW-Map as the machine learning models attempted to learn the intricate  
475 relationship between the HGFs and GWL thereby capturing the complex hydrogeological

476 environment in those areas.

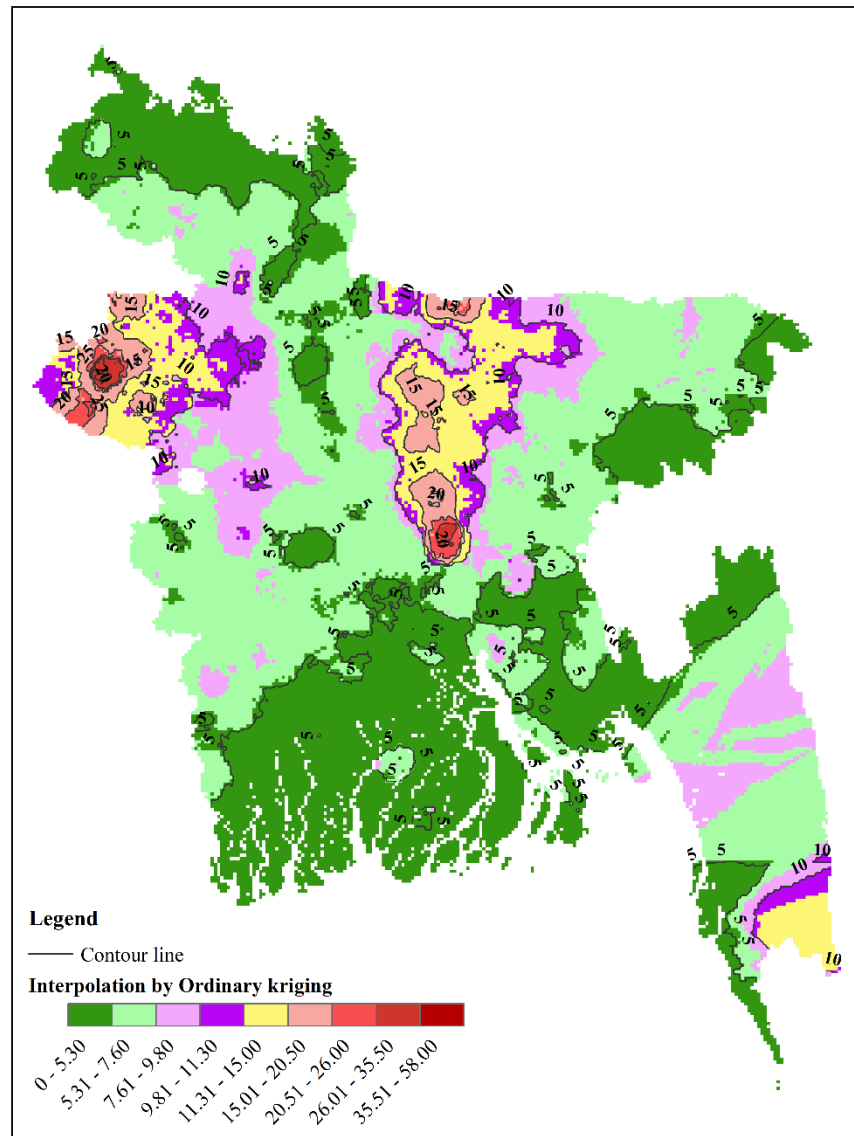


Figure 8: Prediction of annual maximum GWL values that occur in April for Bangladesh by ordinary kriging approach using the same training samples in 2x2km resolution grid.

477 While we have already discussed the peculiarity of Dhaka (Dupi Tila formation) and Barind area,  
478 a brief discussion is also in order including the CHT area. As is evident from the GW-Map, our  
479 machine learning models seem to have predicted deeper GWL depths for Dhaka, Barind and  
480 Chittagong Hill Tracts (CHT) under the same set of constraints when compared to the OK method

481 and this phenomenon (i.e., deeper GWL depths) is most likely accurate as these three particular  
482 regions are well known for their high vulnerability to water crises. Dhaka and Barind's GWL has  
483 deepened owing to high groundwater abstraction for urban water supplies and irrigation,  
484 respectively. On the other hand, the dominant shale/clay materials of CHT is what limits the  
485 recharge in the subsurface geologic formation and causes higher contour with the groundwater  
486 depth. Since there are no samples in the training set with GWL values in the CHT area (due to the  
487 absence of observation wells therein), the OK method failed miserably to predict the GWL in those  
488 areas (as is evident from the OK-GW-Map), whereas the GW-Map reveals that our models seem  
489 to have adequately captured the complex hydrogeological phenomenon in those area.

490 Our study has inherited the limitations of any machine learning model particularly in the context  
491 of the available dataset. The tools and algorithms based on AI and ML are never 100% accurate  
492 and the accuracy usually largely depends on the data- both in terms of quality and quantity.  
493 Therefore, the output of these approaches must be interpreted wisely and cautiously, specifically  
494 where assessment of the dynamic nature of GWL and the spatio-temporal changes are to be taken  
495 into account.

## 496 **5. Conclusion**

497 The ratio of suction mode and force mode abstraction has been significantly changing since the  
498 green revolution started in Bangladesh during the eighties. Yet, government organizations like  
499 DPHE still suggests pumping technology based on the lowest water table declination forecasting  
500 study conducted in 1990 (DPHE 2008), which seems outdated. Therefore, how much withdrawal  
501 can really be sustainable with which mode of pumping technology has now become a crucial  
502 question for management purposes in many parts of the country. Other developing agrarian  
503 countries like India, Vietnam, etc., are no exception. On the other hand, groundwater data

504 collection network density, i.e., standard resolution in Bangladesh is not adequate to forecast  
505 groundwater status at the village, or even union level. To this end, our machine learning models  
506 could be instrumental in answering such and other relevant questions. Furthermore, we believe  
507 that the outcome of this study can aid the policymakers in formulating policies for ensuring  
508 sustainable groundwater management. The output of this study will also be instrumental to the  
509 policy/decision makers to mark suitable locations for drilling production wells, which, in the  
510 sequel, will help farmers reduce the extra unnecessary well construction costs.

## 511 **DECLARATIONS**

### 512 **Funding**

513 This work is part of the project titled ‘Development of IoT enabled data logger to monitor  
514 groundwater and analysis of the collected data’ under the innovation fund of ICT Division,  
515 Bangladesh. It is further supported by AI for Earth Grant for a project titled “GWMap: Applying  
516 Machine Learning to map groundwater levels in Bangladesh”.

### 517 **Conflicts of interest/Competing interests**

518 None to be declared.

### 519 **Availability of data and material (data transparency)**

520 All data are available through the appropriate institutes.

### 521 **Code availability (software application or custom code)**

522 The code will be made available through github/equivalent repository.

523

524 **Authors' contributions**

- 525 Zzaman: Data curation, Formal analysis, Validation, Visualization, Writing - original draft.  
526 Nowreen: Conceptualization, Methodology, Data curation, Formal analysis, Supervision,  
527 Writing - review & editing. Khan: Methodology, Formal analysis, Validation.  
528 Islam: Methodology, Formal analysis, Validation.  
529 Ibtehaz: Methodology, Formal analysis, Validation.  
530 Saifur Rahman: Conceptualization, Methodology, Investigation. Anwar Zahid: Data curation,  
531 validation.  
532 Farzana: Data curation, validation.  
533 Sharmin: Data curation, validation.  
534 Sohail Rahman: Conceptualization, Methodology, Supervision, Writing - review & editing.

535

536 **References**

- 537 Abdollahi, S., Pourghasemi, H. R., Ghanbarian, G. A., & Safaeian, R. (2019). Prioritization of  
538 effective factors in the occurrence of land subsidence and its susceptibility mapping using  
539 an SVM model and their different kernel functions. *Bulletin of Engineering Geology and*  
540 *the Environment*, 78(6), 4017–4034. <https://doi.org/10.1007/s10064-018-1403-6>  
541 Al-Abadi, A. M., Al-Temmeme, A. A., & Al-Ghanimy, M. A. (2016). A GIS-based combining  
542 of frequency ratio and index of entropy approaches for mapping groundwater availability  
543 zones at Badra–Al Al-Gharbi–Teeb areas, Iraq. *Sustainable Water Resources Management*,  
544 2(3), 265–283. <https://doi.org/10.1007/s40899-016-0056-5>  
545 Alam, M. K., Hasan, K. M. S., & Khan, M. R. (1990). Geological map of Bangladesh. United  
546 States Geological Survey Bangladesh, Government of Bangladesh. Retrieved from.  
547 Althuwaynee, O. F., Pradhan, B., Park, H.-J., & Lee, J. H. (2014). A novel ensemble bivariate

548 statistical evidential belief function with knowledge-based analytical hierarchy process and  
549 multivariate statistical logistic regression for landslide susceptibility mapping. *CATENA*,  
550 *114*, 21–36. <https://doi.org/10.1016/j.catena.2013.10.011>

551 Altman, D. G., & Bland, J. M. (1994). Diagnostic tests. 1: Sensitivity and specificity. *BMJ:*  
552 *British Medical Journal*, *308*(6943), 1552.

553 Arabameri, A., Lee, S., Tiefenbacher, J. P., & Ngo, P. T. T. (2020). Novel Ensemble of MCDM-  
554 Artificial Intelligence Techniques for Groundwater-Potential Mapping in Arid and Semi-  
555 Arid Regions (Iran). *Remote Sensing*, *12*(3), 490. <https://doi.org/10.3390/rs12030490>

556 Brammer, H. (2012). *Physical geography of Bangladesh*. The University Press Ltd.

557 Breiman, L. (2001). Random forests. *Machine learning*, *45*(1), 5–32.

558 Bricker, S. H., Banks, V. J., Galik, G., Tapete, D., & Jones, R. (2017). Accounting for  
559 groundwater in future city visions. *Land Use Policy*, *69*, 618–630.  
560 <https://doi.org/10.1016/j.landusepol.2017.09.018>

561 Burgess, W. G., Shamsudduha, M., Taylor, R. G., Zahid, A., Ahmed, K. M., Mukherjee, A., et  
562 al. (2017). Terrestrial water load and groundwater fluctuation in the Bengal Basin. *Scientific*  
563 *Reports*, *7*(1), 3872. <https://doi.org/10.1038/s41598-017-04159-w>

564 Chawla, N. V, Bowyer, K. W., Hall, L. O., & Kegelmeyer, W. P. (2002). SMOTE: synthetic  
565 minority over-sampling technique. *Journal of artificial intelligence research*, *16*, 321–357.

566 Dalin, C., Wada, Y., Kastner, T., & Puma, M. J. (2018). Erratum: Corrigendum: Groundwater  
567 depletion embedded in international food trade. *Nature*, *553*(7688), 366–366.  
568 <https://doi.org/10.1038/nature24664>



569 Davis, J., & Goadrich, M. (2006). The relationship between Precision-Recall and ROC curves. In  
570 *Proceedings of the 23rd international conference on Machine learning* (pp. 233–240).

571 DPHE. (2008). *Union Wise Water Technology Mapping, Government of the People's Republic of*  
572 *Bangladesh (GoB), Department of Public Health Engineering (DPHE). Project Director*  
573 *Sanitation, Hygiene and Water Supply Project (GOB - UNICEF) DPHE, Dhaka.*

574 Earth Resources Observation and Science (EROS) Center. (2021). *U.S. Geological Survey.*

575 EPC/MMP. (1991). Dhaka region groundwater and subsidence study. Final Report, Vol.2, main  
576 report, Dhaka WASA.

577 Fawcett, T. (2006). An introduction to ROC analysis. *Pattern Recognition Letters*, 27(8), 861–  
578 874. <https://doi.org/10.1016/j.patrec.2005.10.010>

579 Freedman, D. A. (2005). *Statistical models: theory and practice*. Cambridge University Press.

580 Harvey, C. F., Ashfaque, K. N., Yu, W., Badruzzaman, A. B. M., Ali, M. A., Oates, P. M., et al.  
581 (2006). Groundwater dynamics and arsenic contamination in Bangladesh. *Chemical*  
582 *Geology*, 228(1–3), 112–136. <https://doi.org/10.1016/j.chemgeo.2005.11.025>

583 Hasda, R., Rahaman, M. F., Jahan, C. S., Molla, K. I., & Mazumder, Q. H. (2020). Climatic data  
584 analysis for groundwater level simulation in drought prone Barind Tract, Bangladesh:  
585 Modelling approach using artificial neural network. *Groundwater for Sustainable*  
586 *Development*, 10, 100361. <https://doi.org/10.1016/j.gsd.2020.100361>

587 Hoque, M. A., & Adhikary, S. K. (2020). Prediction of groundwater level using artificial neural  
588 network and multivariate time series models. *5th International Conference on Civil*  
589 *Engineering for Sustainable Development (ICCESD 2020), 7~9 February 2020, KUET,*

590 *Khulna, Bangladesh.*

591 Hossain, M. M., & Zahid, A. (2014). Bangladesh Water Development Board: A bank of  
592 hydrological data essential for planning and design in water sector. In *Proceedings of the*  
593 *2nd International Conference on Advances in Civil Engineering 2014. Chittagong*  
594 *University of Engineering and Technology, Bangladesh, December 2014.* Proceedings of  
595 the 2nd International Conference on Advances in Civil Engineering 2014. Chittagong  
596 University of Engineering and Technology, Bangladesh, December 2014.

597 Husna, N., Bari, S. H., Hussain, M. M., Ur-rahman, M. T., & Rahman, M. (2016). Ground water  
598 level prediction using artificial neural network. *International Journal of Hydrology Science*  
599 *and Technology, 6(4), 371–381.* <https://doi.org/10.1504/IJHST.2016.07934456>

600 Kohavi, R. (1995). A study of cross-validation and bootstrap for accuracy estimation and model  
601 selection. *IJCAI, 14(1), 1137–1145.*

602 Lee, C. F., Li, J., Xu, Z. W., & Dai, F. C. (2001). Assessment of landslide susceptibility on the  
603 natural terrain of Lantau Island, Hong Kong. *Environmental Geology, 40(3), 381–391.*  
604 <https://doi.org/10.1007/s002540000163>

605 Lumley, T., & Lumley, M. T. (2013). Package ‘leaps.’ *Regression Subset Selection. Thomas*  
606 *Lumley Based on Fortran Code by Alan Miller. Available online: [http://CRAN.R-project.](http://CRAN.R-project.org/package=leaps)*  
607 *org/package= leaps (accessed on 18 March 2018).*

608 Machiwal, D., Jha, M. K., & Mal, B. C. (2011). Assessment of groundwater potential in a semi-  
609 arid region of India using remote sensing, GIS and MCDM techniques. *Water resources*  
610 *management, 25(5), 1359–1386.*

611 Miraki, S., Zanganeh, S. H., Chapi, K., Singh, V. P., Shirzadi, A., Shahabi, H., & Pham, B. T.  
612 (2019). Mapping Groundwater Potential Using a Novel Hybrid Intelligence Approach.  
613 *Water Resources Management*, 33(1), 281–302. <https://doi.org/10.1007/s11269-018-2102-6>

614 Nguyen, P. T., Ha, D. H., Nguyen, H. D., Van Phong, T., Trinh, P. T., Al-Ansari, N., et al.  
615 (2020). Improvement of Credal Decision Trees Using Ensemble Frameworks for  
616 Groundwater Potential Modeling. *Sustainability*, 12(7), 2622.  
617 <https://doi.org/10.3390/su12072622>

618 Nowreen, S., Newton, I. H., Zzaman, R. U., Islam, A. K. M. S., Islam, G. M. T., & Alam, M. S.  
619 (2021). Development of potential map for groundwater abstraction in the northwest region  
620 of Bangladesh using RS-GIS-based weighted overlay analysis and water-table-fluctuation  
621 technique. *Environmental Monitoring and Assessment*, 193(1), 24.  
622 <https://doi.org/10.1007/s10661-020-08790-5>

623 Oke, S. A., & Fourie, F. (2017). Guidelines to groundwater vulnerability mapping for Sub-  
624 Saharan Africa. *Groundwater for Sustainable Development*, 5, 168–177.  
625 <https://doi.org/10.1016/j.gsd.2017.06.007>

626 Powers, D. M. W. (2020). Evaluation: from precision, recall and F-measure to ROC,  
627 informedness, markedness and correlation. *arXiv preprint arXiv:2010.16061*.

628 Qureshi, A. S., Ahmed, Z., & Krupnik, T. J. (2014). *Groundwater management in Bangladesh:  
629 an analysis of problems and opportunities*. Cereal Systems Initiative for South Asia  
630 Mechanization and Irrigation (CSISA-MI) Project, Research Report No. 2., Dhaka,  
631 Bangladesh: CIMMYT.

632 Razandi, Y., Pourghasemi, H. R., Neisani, N. S., & Rahmati, O. (2015). Application of analytical

633 hierarchy process, frequency ratio, and certainty factor models for groundwater potential  
634 mapping using GIS. *Earth Science Informatics*, 8(4), 867–883.  
635 <https://doi.org/10.1007/s12145-015-0220-8>

636 Salam, R., Towfiqul Islam, A. R. M., & Islam, S. (2020). Spatiotemporal distribution and  
637 prediction of groundwater level linked to ENSO teleconnection indices in the northwestern  
638 region of Bangladesh. *Environment, Development and Sustainability*, 22(5), 4509–4535.  
639 <https://doi.org/10.1007/s10668-019-00395-4>

640 Salem, G. S. A., Kazama, S., Shahid, S., & Dey, N. C. (2018). Impacts of climate change on  
641 groundwater level and irrigation cost in a groundwater dependent irrigated region.  
642 *Agricultural Water Management*, 208, 33–42. <https://doi.org/10.1016/j.agwat.2018.06.011>

643 Sameen, M. I., Pradhan, B., & Lee, S. (2019). Self-Learning Random Forests Model for  
644 Mapping Groundwater Yield in Data-Scarce Areas. *Natural Resources Research*, 28(3),  
645 757–775. <https://doi.org/10.1007/s11053-018-9416-1>

646 Sarkar, B. C., Deota, B. S., Raju, P. L. N., & Jugran, D. K. (2001). A Geographic Information  
647 System approach to evaluation of groundwater potentiality of Shamri micro-watershed in  
648 the Shimla Taluk, Himachal Pradesh. *Journal of the Indian Society of Remote Sensing*,  
649 29(3), 151–164. <https://doi.org/10.1007/BF02989927>

650 Shahid, S. (2008). Spatial and temporal characteristics of droughts in the western part of  
651 Bangladesh. *Hydrological Processes*, 22(13), 2235–2247. <https://doi.org/10.1002/hyp.6820>

652 WARPO. (2000). *Draft Development Strategy (DDS), Estimation of groundwater resources,*  
653 *Annex-C, Appendix 6, National Water Management Plan, Water Resources Planning*  
654 *Organization, Ministry of Water Resources.*

655 Wischmeier, W. H., & Smith, D. D. (1978). *Predicting rainfall erosion losses: a guide to*  
656 *conservation planning*. US Department of Agriculture, Washington, D.C.

657 Yamamoto, J. K. (2000). An alternative measure of the reliability of ordinary kriging estimates.  
658 *Mathematical Geology*, 32(4), 489–509. <https://doi.org/10.1023/A:1007577916868>

659 Zhou, T., Wang, F., & Yang, Z. (2017). Comparative analysis of ANN and SVM models  
660 combined with wavelet preprocess for groundwater depth prediction. *Water*, 9(10), 781.

661 Zou, H., & Hastie, T. (2005). Regularization and variable selection via the elastic net. *Journal of*  
662 *the royal statistical society: series B (statistical methodology)*, 67(2), 301–320.

663